The oncogenic and druggable hPG80 (Progastrin) is overexpressed in multiple cancers and detected in the blood of patients

Benoit You, Frédéric Mercier, Eric Assenat, Carole Langlois-Jacques, Olivier Glehen, Julien Soulé, Léa Payen, Vahan Kepenekian, Marie Dupuy, Fanny Belouin, et al.

EBioMedicine 51 (2020) 102574

Contents lists available at ScienceDirect

EBioMedicine

journal homepage: www.elsevier.com/locate/ebiom

Research paper

The oncogenic and druggable hPG80 (Progastrin) is overexpressed in multiple cancers and detected in the blood of patients

Benoit You[a,b,r], Frédéric Mercier[c], Eric Assenat[d], Carole Langlois-Jacques[e,f,g,h], Olivier Glehen[i,j], Julien Soulé[c], Léa Payen[k,l], Vahan Kepenekian[i], Marie Dupuy[d], Fanny Belouin[c], Eric Morency[c], Véronique Saywell[c], Maud Flacelière[c], Philippe Elies[m], Pierre Liaud[c], Thibault Mazard[n,o], Delphine Maucort-Boulch[e,f,g,h], Winston Tan[p], Bérengère Vire[c], Laurent Villeneuve[a,q,r], Marc Ychou[n,o], Manish Kohli[p], Dominique Joubert[s], Alexandre Prieur[s,*]

[a] Hospices Civils de Lyon, Lyon, France
[b] Centre d'Investigation de Thérapeutiques en Oncologie et Hématologie de Lyon (CITOHL), Groupe des Investigateurs Nationaux pour les Cancers de l'Ovaire et du sein (GINECO), Institut de Cancérologie des Hospices Civils de Lyon (IC-HCL), Lyon, France
[c] Eurobiodev, 2040 avenue du Père Soulas, 34000, Montpellier, France
[d] Department of Medical Oncology, CNRS UMR 5535St-Eloi University Hospital-Montpellier School of Medicine, 80, Avenue Augustin Fliche 34295, Montpellier, France
[e] Service de Biostatistique, Bioinformatique, Pôle Santé Publique, Hospices Civils de Lyon, 69424, Lyon, France
[f] Université de Lyon, F-69000, Lyon, France
[g] Université Lyon 1, F-69100, Villeurbanne, France
[h] CNRS, UMR5558, Laboratoire de Biométrie et Biologie Évolutive, Équipe Biostatistique-Santé, F-69100 Villeurbanne, France
[i] General and Oncologic Surgery Department, Lyon Sud University Hospital, France
[j] EMR UCBL/HCL 3738, Université Claude Bernard Lyon 1, Lyon, France
[k] Laboratoire de Biochimie et Biologie Moleculaire, Institut de Cancérologie des Hospices Civils de Lyon (IC-HCL), France
[l] CITOHL, Centre Hospitalier Lyon-Sud, Lyon, France
[m] Plateforme Imagerie Médicale, Univ de Bretagne occidentale, Brest, France
[n] Medical Oncology Unit, Institut régional du Cancer de Montpellier (ICM), Val d'Aurelle, 208 Avenue des Apothicaires, 34298, Montpellier Cedex 5, France
[o] IRCM, Inserm, Univ Montpellier, ICM, Montpellier, France
[p] Division of Medical Oncology, Department of Oncology, Mayo Clinic, Rochester, MN, USA
[q] Hospices Civils de Lyon, Unité Recherche Clinique Pôle de Santé Publique, Lyon, France
[r] EMR UCBL/HCL 3738, Université Claude Bernard Lyon, Lyon, France
[s] ECS-Progastrin, Chemin de la Meunière 12, 1008 Prilly, Switzerland

ARTICLE INFO

Article History:
Received 11 October 2019
Revised 21 November 2019
Accepted 21 November 2019
Available online 24 December 2019

Keywords:
Progastrin
Cancer
Therapy
Blood biomarker
Monitoring
hPG80

ABSTRACT

Background: In colorectal cancer, hPG80 (progastrin) is released from tumor cells, promotes cancer stem cells (CSC) self-renewal and is detected in the blood of patients. Because the gene *GAST* that encodes hPG80 is a target gene of oncogenic pathways that are activated in many tumor types, we hypothesized that hPG80 could be expressed by tumors from various origins other than colorectal cancers, be a drug target and be detectable in the blood of these patients.

Methods: hPG80 expression was monitored by fluorescent immunohistochemistry and mRNA expression in tumors from various origins. Cancer cell lines were used in sphere forming assay to analyze CSC self-renewal. Blood samples were obtained from 1546 patients with 11 different cancer origins and from two retrospective kinetic studies in patients with peritoneal carcinomatosis or hepatocellular carcinomas. These patients were regularly sampled during treatments and assayed for hPG80.

Findings: We showed that hPG80 was present in the 11 tumor types tested. In cell lines originating from these tumor types, hPG80 neutralization decreased significantly CSC self-renewal by 28 to 54%. hPG80 was detected in the blood of patients at significantly higher concentration than in healthy blood donors (median hPG80: 4.88 pM versus 1.05 pM; $p < 0.0001$) and shown to be correlated to *GAST* mRNA levels in the matched tumor (i.e., lung cancers, Spearman $r = 0.8$; $p = 0.0023$). Furthermore, we showed a strong association between longitudinal hPG80 concentration changes and anti-cancer treatment efficacy in two independent retrospective studies. In the peritoneal carcinomatosis cohort, median hPG80 from inclusion to the post-operative period decreased from

* Corresponding author.
E-mail address: a.prieur@ecs-progastrin.com (A. Prieur).

https://doi.org/10.1016/j.ebiom.2019.11.035

5.36 to 3.00 pM ($p < 0.0001$, $n = 62$) and in the hepatocellular carcinoma cohort, median hPG80 from inclusion to remission decreased from 11.54 pM to 1.99 pM ($p < 0.0001$, $n = 63$).
Interpretation: Because oncogenic hPG80 is expressed in tumor cells from different origins and because circulating hPG80 in the blood is related to the burden/activity of the tumor, it is a promising cancer target for therapy and for disease monitoring.
Fundings: ECS-Progastrin.

Research in context

Evidence before study

The National Cancer Institute recently highlighted the need for biomarkers to improve early detection of cancers, monitor treatment effects and detect disease relapses. Therefore, the identification of a new tumor blood-based marker with broad expression across tumor types might have a significant impact on diagnostic and follow-up of patients. hPG80 (progastrin) was shown to be over-expressed in human colorectal tumor cells. Interestingly, *GAST* is a direct target of the Wnt/ß-catenin/Tcf4 oncogenic pathway. Since this pathway is activated in many other cancers and plays a major function in cancer stem cells survival, we hypothesized that hPG80 (i) might be expressed by other types of cancers, and would be present in the blood of patients with tumors different from colorectal cancers and (ii) might be a drug target for various type of cancers.

Added value of this study

Here we show that hPG80 is expressed by the tumor and present in the blood of 11 different types of cancer patients. Two retrospective kinetic studies where blood samples were collected regularly from cancer patients undergoing different treatments revealed strong associations between longitudinal hPG80 concentrations and anti-cancer treatment efficacy. We provide data showing the decrease of hPG80 after surgery in a cohort of patients with peritoneal involvements from gastrointestinal cancers, treated with peri-operative chemotherapy regimens and cytoreductive surgery. We also show the correlation between hPG80 levels and standard imaging in a cohort of patients with hepatocellular carcinoma, managed with local or systemic treatments, including patients with no detectable levels of alpha-fetoprotein. Finally, we show that targeting hPG80 with our humanized antibody decreases self-renewal capacity of cancer stem cells from various origins.

Implications of all available evidence

The technology we developed to detect hPG80 in the blood is robust, reliable and inexpensive, making this test easy to implement by oncologists. This technology could be used to improve early cancer diagnosis and treatment efficacy monitoring. Furthermore, in this study we show that our anti-hPG80 therapeutic antibody, that was initially found to target the Wnt pathway and decrease self-renewal capacity in cancer stem cells from colorectal cancer, is envisioned to have the same effect on tumors from other origins.

1. Introduction

Physiologically, hPG80 (progastrin), an 80 amino acid protein, is the precursor of the gastrointestinal hormone gastrin. It is synthetized by gastric antrum G cells, and then processed into gastrin by multiple enzymatic processes [1]. In pathological conditions, the *GAST* gene, which encodes hPG80, was shown to be over-expressed in human colorectal tumor cells, leading to hPG80 accumulation [2,3]. As hPG80 is either unprocessed or poorly processed into gastrin, it is released from the tumor cells and becomes detectable in the blood of colorectal cancer (CRC) patients [4,5].

Initially believed to be biologically inactive, hPG80 was shown to participate in some features of a tumor, such as the disruption of cell−cell junctions [6], cell proliferation [7], inhibition of apoptosis [8], regulation of cancer stem cells [9], and angiogenesis [10]. In addition, our team demonstrated that targeting hPG80 with a specific antibody promotes apoptosis, decreases proliferation and migration/invasion of human colorectal cancer cells, and inhibits self-renewal of colon cancer stem cells (CSC), as well as Wnt-driven tumorigenesis in mice [5]. Interestingly, *GAST* is a direct target of the Wnt/ß-catenin/Tcf4 oncogenic pathway [3]. Since this pathway is activated in many other cancers and plays a major function in cancer stem cells survival [11], we hypothesized that hPG80 might be expressed by other types of cancers, and would be present in the blood of patients with tumors different from colorectal cancers.

In the present study, we examined the *in situ* expression of hPG80 in the tissues obtained from the surgical resections of patients ($n = 19$) with eight tumor types. We compared hPG80 expressions in the tumor cells with those of normal adjacent tissues. Given the critical role of hPG80 as a pro-oncogenic factor, we evaluated the anti-oncogenic efficacy of anti-hPG80 antibodies on *in vitro* cultured cell lines from 7 cancer types, with survival and sphere formation assays. Furthermore, the blood samples from 1546 patients with 11 different types of cancers (breast, uterus, ovarian, prostate, kidney, colorectal, pancreas, esophagus/stomach, liver, skin melanoma and lung) and from 557 healthy blood donors were assayed for hPG80. Finally, the hPG80 longitudinal kinetics during treatments in cancer patients were assessed in 2 retrospective studies to investigate the relationships between cancer activity and hPG80 titers.

2. Materials and methods

2.1. Tumor tissue samples for immunohistochemistry and GAST mRNA expression analyzes

Human tissue samples, obtained by surgical resection, were collected from a tissue bank (Tissue bank, Tumorothèque, CHRU Brest, France). They involved 19 patients with the following cancer origins: colon, kidney, pancreas, liver, breast, ovary, lung, and stomach. The tissue samples were preserved at −80 °C until sectioned with a cryostat, and stored at −40 °C. Paired samples of tumor and adjacent tissues were assessed for hPG80 expression. Confocal images from 19 patients are shown in the figures of this paper. The clinical characteristics and tumor types of these 19 patients are presented on Table S1. For 10 of them, the adjacent tissues were also available.

In addition to the abovementioned tissues, some additional tissues were collected to assess the *GAST* mRNA expression levels in independent cohorts, including: the primary tumor samples from 12 colorectal cancer (CRC) patients matched with metastasis tumor tissues (Tissue bank, Tumorothèque, ICM Montpellier, France); the primary tumor samples from 14 patients with hepatocellular

carcinoma (HCC) tissues (Tissue bank, Tumorothèque, Institut Cochin, France); the primary tumor samples from 15 patients with lung cancers, including 11 with matched tissues and blood samples (Tissue For Research Ltd, Spectrum Health System, Grand Rapids, Michigan, USA).

2.2. Blood samples from cancer patients for circulating titer analyzes

The blood samples from non-fasting 1546 patients with 11 different types of cancers were used for measuring their hPG80 blood concentrations (breast, uterus, ovarian, prostate, kidney, colorectal, pancreas, esophagus/stomach, liver, skin melanoma and lung). The datasets and blood samples originated from various different biobanks. Plasma were sampled at different times of patient disease managements.

Blood samples from CRC patients were obtained from the SIRIC (*Site de Recherche Intégrée sur le Cancer*) Montpellier Cancer (Montpellier, France), from the French prospective BIG-RENAPE project database (Lyon, France, NCT02823860) and from Tissue For Research Ltd (Spectrum Health System, Grand Rapids, Michigan, USA). The hepatocellular carcinoma (HCC) cohort came from the CHU (Centre Hospitalier Universitaire) Montpellier biobank (BB-0033-00031; the "Liverpool" collection; DC 2014-2328; AC 2014-2335; Montpellier, France). The metastatic kidney cancer cohort and the metastatic hormone sensitive prostate cancer, both came from the Mayo Clinic biobank (Rochester, NY, USA). All other samples were from Tissue For Research Ltd (Spectrum Health System, Grand Rapids, Michigan, USA).

Moreover, the longitudinal changes in hPG80 concentrations in cancer patients managed with different anti-cancer treatments were assessed in two retrospective kinetic studies, as a way of investigating the relationships between hPG80 blood levels and cancer activity. PRO-RENAPE was a cohort of 194 patients with peritoneal involvements from gastrointestinal cancers, treated with peri-operative chemotherapy regimens and cytoreductive surgery. The patients were extracted from the French prospective BIG-RENAPE project database (Lyon, France, NCT02823860). Blood samples were collected at inclusion (n = 194) and between 8 and 24 h after cytoreductive surgery, performed with or without hyperthermic intraperitoneal chemotherapy (HIPEC) (n = 85).

PRO-HCC was a cohort of 84 patients with HCC, managed with local or systemic treatments, including molecular targeted agents ("Liverpool" collection).

The following patient covariates were retrieved from the datasets: age and inflammation status with C-reactive protein (CRP) levels, disease stages according to either the American Joint Committee on Cancer (AJCC) guidelines (7th Edition 2010), or the Barcelona clinic liver cancer (BCLC) for HCC.

All patients (in the cancer and control groups) provided consent for research on their blood samples, in line with international regulations and ICH GCP (International Conference on Harmonization-Good Clinical Practice).

2.3. The control cohort

The blood samples from non-fasting 557 healthy donors, aged 18−70 years, were obtained from the French blood agency (*Etablissement Français du Sang*) to build the control group. Although the agency requires that blood donors attest to be healthy, with no known history of cancer, we could not exclude the possibility that they had a cancer at the time of donation as the main risk factor for developing a cancer is age [12].

2.4. Cell lines

The following human cell lines were used: colorectal, T84; lung, NCI-H358; ovarian, SKOV3; gastric, AGS; esophageal, OE33; hepatoma, Huh7 and breast, MCF7; all of them being obtained from the American Type Culture Collection (ATCC; Rockville, MD, USA). T84 were cultured in DMEM-F12 medium (PAN-Biotech). SKOV3, OE33, NCI-H358 were cultured in RPMI medium (PAN-Biotech). MCF-7 were cultivated in MEM Eagle with EBSS medium (PAN-Biotech). AGS were cultivated in F12-K medium (Mediatech, Inc.) and Huh7 were cultivated in α-MEM medium (Sigma-Aldrich) supplemented with non-essential amino acids (Gibco) and sodium pyruvate (PAN-Biotech). All culture medium were supplemented with 10% foetal calf serum (PAN-Biotech) and 1% v/v penicillin/streptomycin (PAN-Biotech). Absence of mycoplasma infection was confirmed by regular testing.

2.5. Immunofluorescence IHC

Immunofluorescence IHC was performed as previously described [13]. Briefly, human frozen sections were unfrozen, fixed with 4% PFA for 10 min, permeabilized with Triton X100, incubated simultaneously with the primary antibodies, i.e. one of the antibodies directed against hPG80, made in rabbit, and directed against the C-terminal or the N-terminal parts of hPG80, and one antibody directed against heparin sulfate proteoglycans (10E4 epitope, Amsbio, Abingdon, UK), then incubated with secondary antibodies (anti-rabbit conjugated to AlexaFluor-647 and anti-mouse IgM conjugated with AlexaFluor-565, both from Merck, Lyon, France). Human tissues autofluoresce through the entire visible spectrum but not in the near infrared wavelength, as exemplified in Fig. S1A−C. This is due to large quantities of elastin in the connective tissues, and of lipofuchsin in the lysosomes of macrophages. In order to address this problem, we visualized hPG80 labeling with secondary antibodies conjugated to AlexaFluor-647 (near infrared). The green channel of the confocal microscope was also turned on during recordings, without antibody labeling in this wavelength, to independently record autofluorescence of the tissue samples. Therefore, the autofluorescence appeared with white color whereas the specific hPG80 labeling was visualized with the red color only (Fig. S1D). The sections were counterstained with bisbenzimide to visualize the cell nuclei. Results were recorded with a Zeiss confocal laser scanning microscope at the PIMM facility (Plateforme d'Imagerie et de Mesures en Microscopie) of the University of Brest.

2.6. Controls of labeling/antibody specificity for IHC

Control experiments were carried out according to common standards to assess the specificity of the hPG80 labeling by IHC [14]. Additional IHC labelings were processed as described above, but with either different primary antibodies directed against hPG80 (Fig. S2A-B), omission of the primary antibodies (Fig. S2C−D), omission of the primary and secondary antibodies (Fig. S2E-H), or pre-absorption of the anti-hPG80 antibodies with the recombinant protein hPG80 (Fig. S2I and J). The recombinant hPG80 was produced in E. coli BL21 Star (DE3) strain (Institut Pasteur). A 50-fold excess of the recombinant hPG80 protein was incubated with the antibodies prior to incubating frozen sections (Fig. S2G and H). All tests were successful. The N-terminal and the C-terminal antibodies generated similar labelings, no signal -besides autofluorescence- was detected without primary and/or secondary antibodies, and the hPG80 immunoreactivity was quasi-absent in the pre-absorption experiments (Fig. S2).

2.7. RNA extraction from tissues, reverse transcription, and qPCR

Lysis of tumor samples stored in liquid nitrogen was achieved using GentleMACS Octo Dissociator (Miltenyi Biotec). The mRNA extraction was performed with RNeasy Mini Kit (QIAGEN) according to the manufacturer's instructions. Retrotranscription was performed on 1 μg mRNA with Primescript RT Mastermix (Takara) according to the manufacturer's instructions on a MasterCycler ep Gradient (Eppendorf) machine. Finally, quantitative PCR was performed on

2 μL of cDNA with the Sybr Premix ExTaq kit (Takara) according to the manufacturer's instructions in white skirted Twin. The sequences of the qPCR primers (Sigma) were: hGAST-F (5′- CCACACCTCGTGGCAGAC -3′), hGAST-R (5′- TCCATCCATCCATAGGCTTC -3′), hGAPDH-F (5′- CATGAGAAGTATGACAACAGCCT -3′), hGAPDH-R (5′- AGTCCTTCCACGATACCAAAGT -3′), hHPRT1-F (5′-CTTTGCTTTCCTTGGTCAGG-3′), and hHPRT1-R (5′-TCAAATCCAACAAAGTCTGGC-3′); hEEF1A1-F (5′-ATGCTGCCATTGTTGATATG-3′), hEEF1A1-R (5′-ATTCATTTAGCCTTCTGAGC-3′); hACTB-F (5′-GATCAAGATCATTGCTCCTC-3′) and hACTB-R (5′-TTGTCAAGAAAGGGTGTAAC-3′).

2.8. *Survival assays* in vitro *cultured cells*

Survival assays were performed as described by Prieur et al. [5]. Briefly, 100,000 (for T84), 300,000 (for NCI-H358) and 120,000 (for SKOV3) single cell suspensions were homogeneously seeded in 6-well plates (NUNC 055426) in complete medium and incubated for 7 h at 37 °C in a 5% CO_2 atmosphere. After cell adherence, the medium was removed and the wells refilled with serum-free culture medium for overnight incubation. The treatments then began by exchanging the medium for fresh serum-free medium containing the antibodies of interest at the indicated concentrations. The treatment was renewed once daily (for SKOV3) or twice daily (for NCI-H358 and T84) for 48 h, before dissociating the cells and assaying the concentration of propidium-positive and -negative cells using a C6 Accuri flow cytometer (Becton-Dickinson). Cell counts at the start of treatment (T0) were subtracted from test and control cell counts measured at 48 h.

2.9. *Sphere formation assay*

The sphere formation assay was performed as described by Prieur et al. [5]. Spheres were cultivated in Ultra-Low Adherence (ULA) polystyrene flasks or plates (Corning) in M11 medium: DMEM/F12 with Glutamax (Gibco 31331-028), 20 μg/mL insulin (Sigma I0908), 1% N2 supplement (Gibco 17502-048), 20 ng/mL EGF (R&D Systems 236-EG), 10 ng/mL bFGF (R&D Systems 233-FB/CF), 3 mg/mL D-glucose (Sigma 49139), and 1% penicillin-streptomycin (PanBiotech P06-07100). Briefly, dissociated cells were seeded with 150 to 700 single cells, for all cell lines tested, per well in 24-well ULA plates with a FACS Aria (Becton-Dickinson) in 500 μL M11 medium per well. The cells were cultivated for 7 to 11 days and treated every 3 to 4 days with the antibodies of interest at the indicated concentrations. After 7−11 days at 37 °C in 5% CO_2, each well was photographed by bright-field microscopy (Nikon ECLIPSE TS100, image acquisition with NIS-Element F) and the pictures analyzed by ImageJ (NIH) to count the spheres with a mean diameter >20 μM.

2.10. *Measuring hPG80 in the blood samples*

DxPG80 lab kit (the ELISA assay developed by ECS-Progastrin, Switzerland) was used to measure hPG80 levels in all blood samples according to the manufacturer's instruction. According to the manufacturer, the limit of Detection (LoD) is at a hPG80 concentration of 1.2 pM and the limit of Quantitation (LoQ) is at a hPG80 concentration of 2.3 pM. The inter- and intra-assay coefficients of variation (CV%) is below 10%.

2.11. *Measuring alfa-fetoprotein (AFP) concentrations*

In the HCC cohort, blood AFP concentrations were centrally measured using Cobas E411.

2.12. *Statistical analyzes*

Changes in hPG80 levels over time in the two kinetic cohorts were assessed with the concentrations measured at the main stages of disease management and at relapse/progression if any. Patterns were explored using graphical descriptive figures and statistics. The kinetics of hPG80 and AFP were assessed in the PRO-HCC cohort. Acknowledging the lack of a validated percentage increase to describe blood tumor biomarker progression, a 25% change in hPG80 concentration was arbitrarily selected in the present study. This cut-off was previously reported for prostate-specific antigen (PSA) in prostate cancer [15].

Correlations between covariates and hPG80 levels were measured by Spearman correlation coefficients. Mann−Whitney *U* -tests were used to compare continuous covariates.

Statistical analyzes were performed with two-sided 5% alpha risks, using SAS software (GraphPad Prism version 9.4 for Windows, GraphPad Software, La Jolla California USA, www.graphpad.com.)

3. Results

3.1. *Detection of hPG80 in colorectal tumors by immunofluorescence IHC*

Fluorescence IHC was first conducted in sections of colon cancers where hPG80 is known to be expressed [2,9,16]. Dual immunolabelings for hPG80 (in red), heparan sufates (in green) and cell nuclei counterstaining (in blue) were performed to visualize hPG80 expression and basement membranes (heparan sulfate proteoglycan immunoreactivity, HSPG) in the histological context. Fig. 1(A) shows that hPG80 is primarily expressed in cell clusters within the intestinal glands (arrow and double arrow). These cells were mostly epithelial cells (Fig. 1(A) and (B)), recognizable by their round cell nucleus and by their location within gland-delineating basement membranes (Fig. 1(A), arrowhead). At the subcellular level, hPG80 expression was concentrated in the perinuclear area (Figs. 1(C) and S3). Fig. 1(E) shows that hPG80 was expressed in the cytoplasm revealing a punctuate or granular pattern which suggests the subcellular localization in the organelles. Investigation of hPG80 in other patients with colon cancer confirmed these data (Fig. S3).

Investigation of hPG80 expression in the tissues adjacent to the tumor revealed variations according to the tissue sample. In most patients, adjacent tissue was showing scarce, if any, hPG80 immunoreactivity (Fig. 1(D) and (F)). hPG80 expression was generally found in the stroma (arrowhead), and to a lesser extent in epithelial cells (arrow) (Fig. 1(B)). The stroma displayed cells with various morphologies (compare arrowhead and double arrow) (Fig. 1(D)).

3.2. *Detection of hPG80 in other types of tumors by immunofluorescence IHC*

To assess whether hPG80 is expressed in tumors different from CRC, we carried out experiments with multiple cancer tissues. First, dual immunolabelings for hPG80 (in red), heparan sulfates (in green) as well as nuclear counterstaining (in blue) were performed in primary tumor samples of pancreas, liver and kidney. hPG80 was detected in all tumor tissues, as illustrated in Figs. 2 and S4. A loss of basement membrane integrity was usually associated with cancer patterns (Fig. 2(A), (C) and (E)). The adjacent tissues displayed the typical basement membranes of differentiated tissues, and scarce or absent hPG80 immunoreactivity (Fig. 2(B), (D) and (F)).

Fig. S5 shows hPG80 expression in both epithelial and stromal cells of stomach adenocarcinomas. Epithelial cells (Fig. S5A, arrow) were typically delineated by a basement membrane (double arrow), whereas stromal cells were located in the other side of the basement

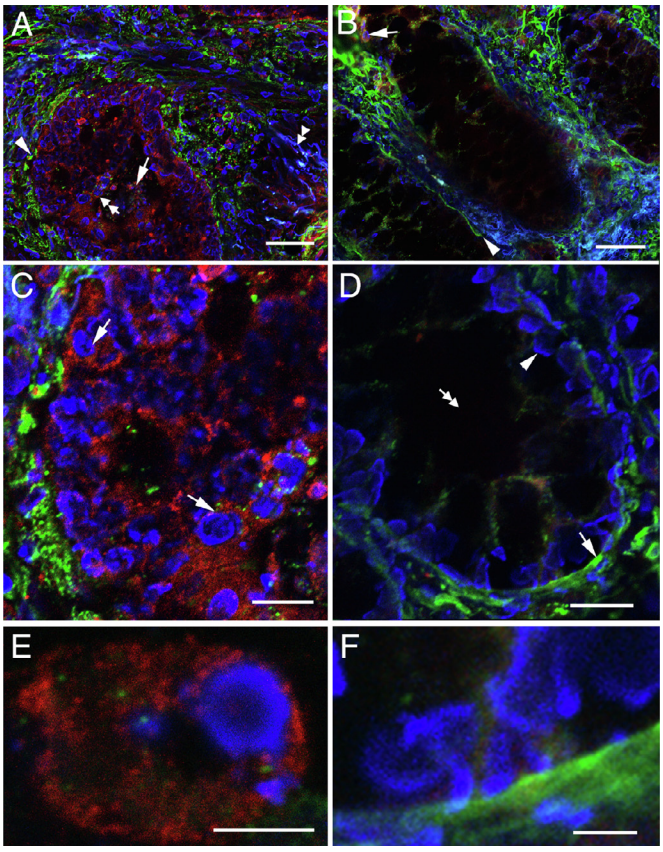

Fig. 1. High expression of hPG80 by tumor cells from colorectal cancer. (A) Confocal image of a tumoral mass showing high expression of hPG80 in colon cancer (patient 6607). The tumor cells expressing hPG80 were visualized with IHC for hPG80 (red). The hPG80-immunoreactive cells were often clustered into masses (arrow) into low-differentiated glands surrounded by disrupted basement membranes (arrowhead, HSPG-immunoreactivity, green). The double arrowhead indicates autofluorescence in the connective tissue (blue), which contrasts with cell nuclear counterstaining with bisbenzimide (blue, double arrow). (B) The tissue peripheral to the tumor mass showed scarce hPG80-immunoreactive cells in the connective tissue (arrow) and linear basement membranes (arrowhead). (C) Magnified field of the area indicated by an arrowhead in (A) showing the perinuclear location of hPG80-immunoreactivity (arrows). (D) Magnified field of the peripheral tissue showing the linear basement membrane (arrow), nuclei of epithelial cells (arrowhead) and the lumen of the gland (double arrow). (E) Highly-magnified field showing one cell and the cytoplasmic localization of hPG80. (F) Absence of hPG80-immunoreactive cells in the peripheral tissue. Scale bars: A and B: 50 μm; C and D: 20 μm; E and F: 5 μm.

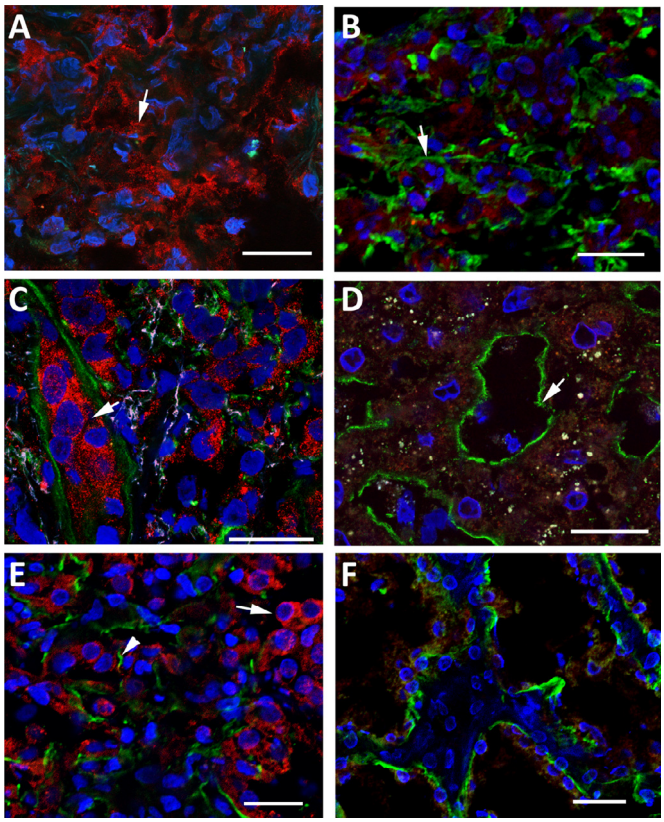

Fig. 2. High expression of hPG80 by tumor cells from kidney, pancreatic and liver cancers. (A) High expression of hPG80 was found in a pancreatic cancer lesion (arrow, patient 1287). HSPG immunoreactivity was not assessed in this sample. (B) The tissues peripheral to the tumor masses were devoid of hPG80-immunoreactive cells. HSPG immunoreactivity (green) showed linear basement membranes (arrow). (C) Typical hPG80 expression in tumors of the liver. hPG80-immunoreactive cells were numerous in the central tumor masses (arrow). Basement membranes were disrupted or inexistent (green, patient 306). (D) Typical organization of basement membranes in tissues peripheral to the tumor masses (arrow). Cells were devoid of hPG80 immunoreactivity. (E) Numerous hPG80-immunoreactive cells were present in the tumor masses of kidney cancers (arrow, patient 3848). Basement membranes were mostly disrupted (arrowhead, HSPG immunoreactivity, green). (F) The normal tissue adjacent to the tumor was devoid of hPG80. Basement membranes were more linear as expected in normal healthy tissues. Scale bars: 25 μm.

membrane (double arrowhead). All images indicate that hPG80 is not expressed in the extracellular matrix (Fig. S5A) – the green and red colors were always separated – but in the cytoplasm. This is clearly illustrated in Fig. S5B (three-dimensional confocal reconstruction). Similarly to colon tumors, hPG80 was often detected in *trabeculae*, i.e. chains of stromal cells (Fig. S5C, arrow) encompassing the tumor mass, and spaning through the adjacent tissues (Fig. S5D, arrow). The adjacent tissue was clearly altered, showing undifferentiated groups of cells without glandular organization (Fig. S5D, double arrow) and basement membranes (Fig. S5D, arrowhead). In patient shown in Fig. S5, the glands of the adjacent tissue showed no hPG80 expression (fig. S5D, arrowhead) whereas numerous ectopic cells expressed hPG80 in the lumen of the glands within the tumor mass (Fig. S5C, arrowhead).

High hPG80 expression was then confirmed in other tumor tissues, from ovary, breast and lung cancers. Strikingly, all tumors displayed many hPG80 immunoreactive cells in the tumor bulk (arrows, Figs. S6, S7 and S8), whereas adjacent tissues were free of hPG80 (Fig. S6D and F).

3.3. *High expression of* GAST *in CRC, hepatocellular carcinoma and lung tumors*

To confirm the high hPG80 expression in tumor cells by another method, RT-PCR analysis of *GAST*, which encodes hPG80, were carried out in a series of primary tumors with matched metastases, surgically removed from patients with CRC, hepatocellular carcinoma (HCC) and lung cancers. We showed the expression of *GAST* in primary tumors and in the matched metastatic tumors from 12 stage IV CRC patients (Fig. 3 (A)). Depending on the patients, the levels of *GAST* in the metastatic lesion cells was either lower (42%), equal (16%) or higher (42%) than in the primary tumors, with a maximum of 30 times higher expression. Compared to the expression in T84 CRC cell line, *GAST* mRNA was also detected in all HCC tumor samples (14/14) with a relative range ranking from 3.95 to 21,277, and 11/15 lung tumor samples with a relative range ranking from 0.06 to 36.37 (Fig. 3(B)–(C)).

3.4. *Anti-hPG80 antibody decreases cell proliferation in tumor cell lines different from CRC*

We assume that aberrant hPG80 expression might be exploited for therapeutic purpose, as already shown in CRC [5] and confirmed

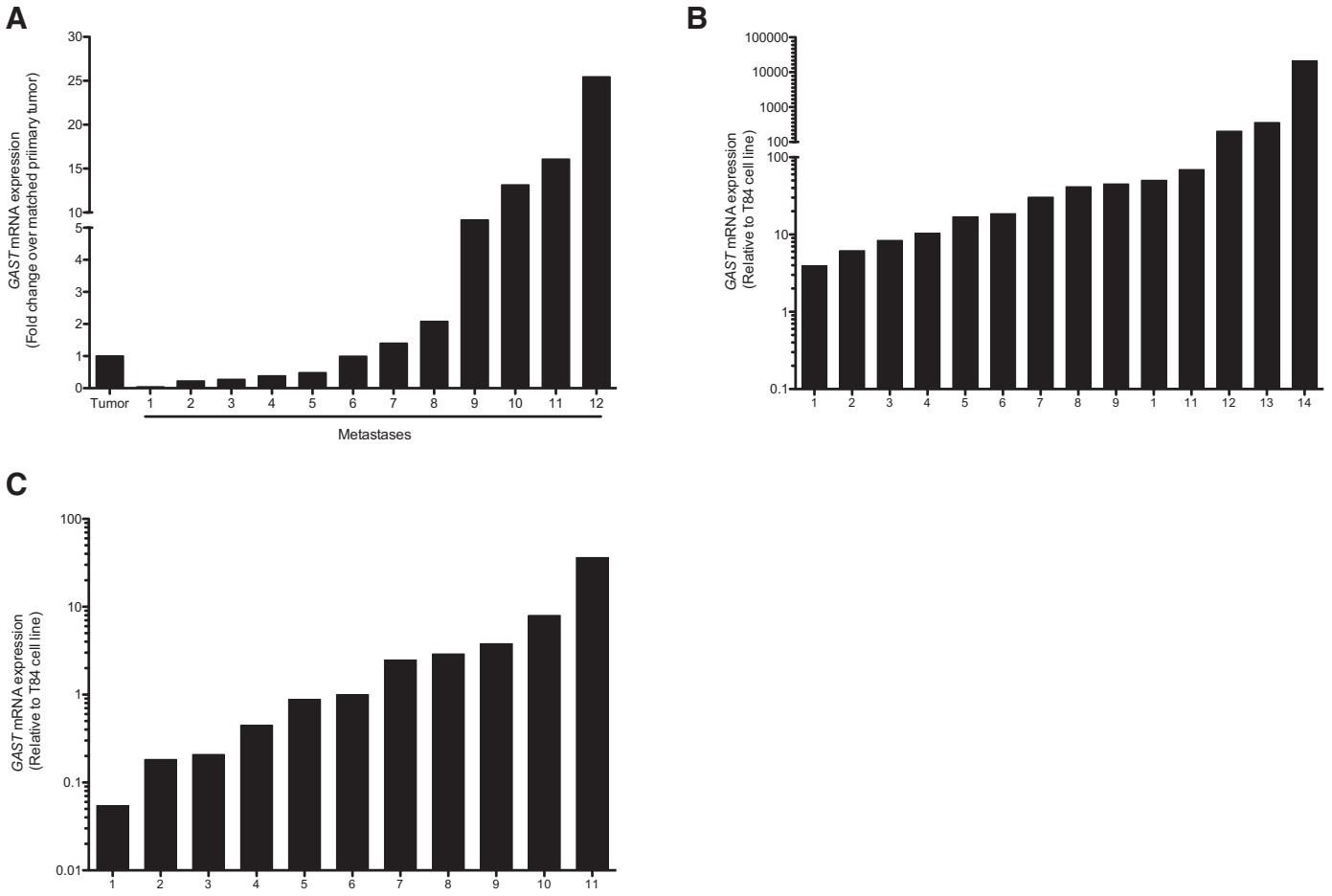

Fig. 3. hPG80 is highly expressed at the RNA levels in tumors of different origins. (A) *GAST* mRNA levels (normalized to *GAPDH*) in primary tumors and corresponding metastases in 12 CRC patients. *GAST* mRNA levels relative to the average level detected in healthy colon tissues. Results are shown as fold change of *GAST* expression in the metastasis over matched primary tumor. (B) *GAST* mRNA levels (normalized to *HPRT*) in 14 patients with liver cancer (hepatocellular carcinoma, HCC) relative to the average level in T84 colorectal cancer cell line. (C) *GAST* mRNA levels (normalized to *ACTB* and *EEF1A1*) in 15 patients with lung cancer relative to the average level in T84 colorectal cancer cell line.

in Fig. S9 (90% decrease of cell growth in T84 CRC cell line). We tested two cell lines from ovarian and lung cancer origins. Accordingly, treatment of human ovarian (SKOV3) cancer cells with a humanized anti-hPG80 antibody induced a significant 96.1% decrease of cell growth, suggesting that hPG80 was not only released by the human ovarian cancer cells, but was also required for the survival of these cells (Fig. S9B). Cell survival was also significantly decreased in NCI-H358 human lung cell line by 32.5% (Fig. S9C). These results provide evidence that hPG80 is able to decrease the survival of tumor cells from different origins.

3.5. Anti-hPG80 antibody decreases sphere formation from tumor cell lines different from CRC

Cancer stem cells (CSCs) are key drivers of tumor progression [17]. CSCs have the ability to form spheres *in vitro* when grown in non-adherent serum-free conditions [18]. Sphere formation assays provide therefore a useful tool to assess the growth and propagation of CSCs in cancer cell lines. To evaluate the effects of anti-hPG80 antibodies on sphere formation, cell lines from six different origins were grown as spheres, and incubated with anti-hPG80 antibodies for 7 to 11 days. As shown in Fig. 4(A), a 40% inhibition of spheres number in the T84 CRC cell line was observed in the presence of anti-hPG80 antibodies. Similar resuts were obtained in the five other cell lines tested, with inhibitions of spheres number by 54.1% for SKOV3 (ovarian), 50.6% for MCF-7 (breast), 37.7% for OE33 (esophageal), 36.7% for Huh-7 (hepatic), and 28% for AGS (gastric) (Figs. 4(B)–(F)), thereby suggesting that hPG80 controls the self-renewal of CSCs originating from various cancers.

3.6. hPG80 was detectable in the blood of patients with various cancer origins

After validating the expression of hPG80 within the tumors, we analyzed the levels of hPG80 in the blood of cancer patients. The cohort was composed of 1546 patients with 11 different cancer origins. These included breast (n = 62); colorectal (n = 305); esophagus/stomach (n = 74); kidney (n = 184); liver (n = 110); lung (n = 60); skin melanoma (n = 38); ovary (n = 44); pancreas (n = 34); prostate (n = 558); uterus (n = 77) (Table 1). When all these cancer types were combined, the median hPG80 concentration was 4.88 pM (IQR 2.02-11.73 pM) (Fig. 5(A) and Table 1). It was significantly higher than the median hPG80 concentration in the control group composed of healthy blood donors (1.05 pM (IQR 0.00–2.92 pM); $p < 0.0001$). Median hPG80 concentration across tumor types varied from 2.50 to 11.65 pM (Fig. 5(B), and Table 1). In both healthy donors and cancer patients, the relationship with age existed, but was moderate (Fig. S10). For the cancer group, the Spearman Rhô = 0.31; for healthy blood donors, the Spearman Rhô = 0.34.

Interestingly, the blood levels of hPG80 correlated with the expression of *GAST* mRNA in the matched tumors of 11 patients with lung cancers (Spearman r = 0.8; p = 0.0023), thereby suggesting

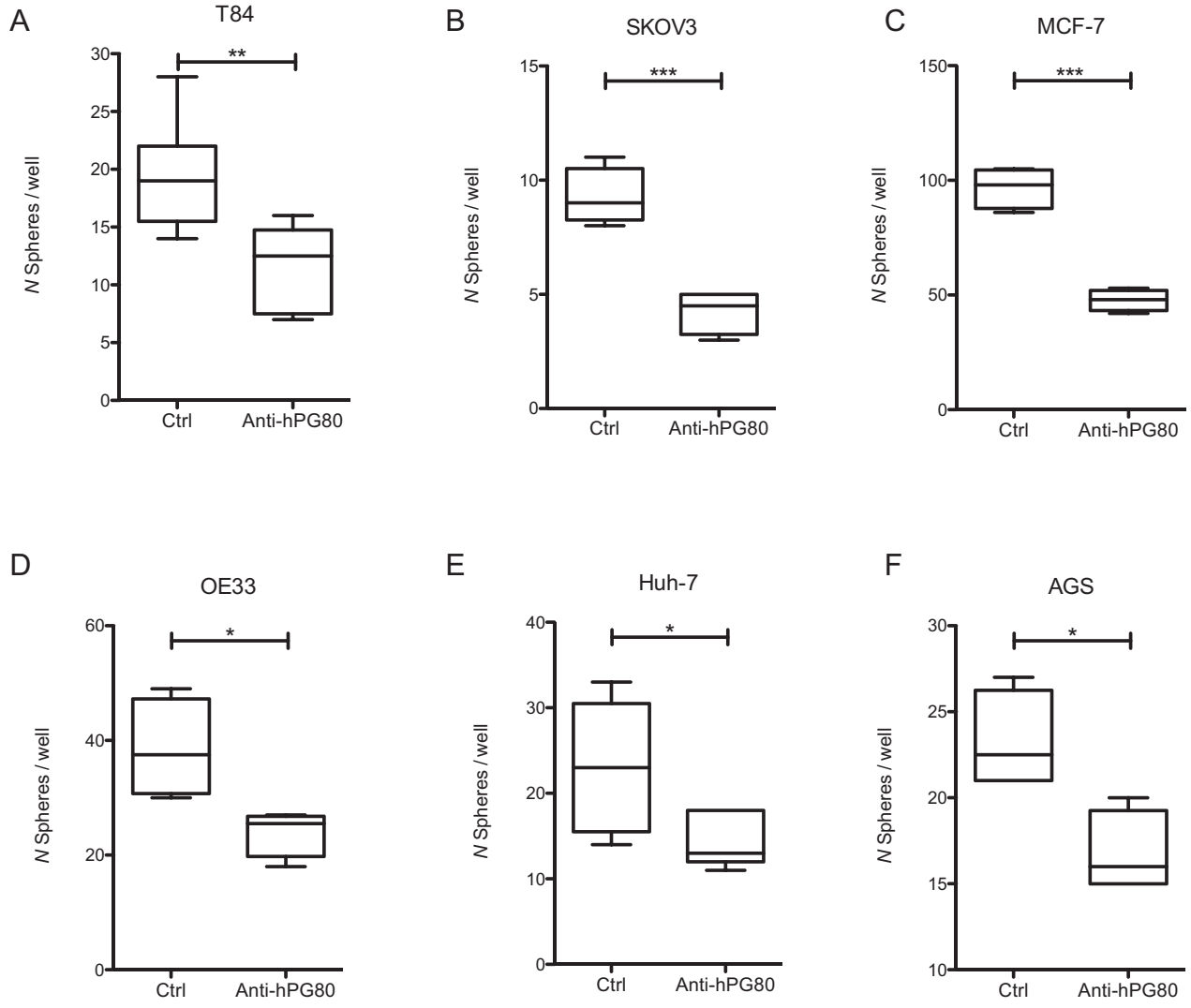

Fig. 4. Anti-hPG80 antibody decreases stem cell frequency. Average number of spheres for T84 (A), SKOV3 (B), MCF-7 (C), OE33 (D), Huh-7 (E) and AGS (F), following treatment with control or anti-hPG80 antibodies (monoclonal or humanized) under ULA conditions. T84 and Huh-7 were treated with 10 μg/ml; SKOV3, OE33 and AGS were treated with 20 μg/ml and MCF-7 were treated with 3 μg/ml of control or anti-hPG80 antibodies. Two-tailed unpaired *t*-test; * $0.01 < p < 0.05$; ** $0.001 < p < 0.01$; *** $p \leq 0.001$.

the tumoral origin of hPG80 detected in the blood of the patients (Fig. 5(C)).

3.7. hPG80 kinetics in patients receiving anti-cancer treatments

In the two kinetic datasets, explorative and descriptive analyzes of concentration versus time curves were performed in order to analyze the impact of cancer treatments on hPG80 levels, as a way of assessing the links between hPG80 levels and tumor activity.

In the PRO-RENAPE cohort, median hPG80 significantly decreased from inclusion to the post-operative period from 3.08 to 1.57 pM (Fig. 6(A)). The individual curves showed that 74.2% of patients had hPG80 titer declines >25%. The remaining patients experienced stable concentrations (16.1% of patients), or hPG80 level increases >25% (9.7% of patients) (Fig. 6(B)). In Fig. 6(B), we performed an individual analysis on 62 patients before and after surgery using Wilcoxon matched pairs test. Patients were stratified in two groups according to the decrease (n = 46, left part of Fig. 6 (B)) and stable or increase (n = 16, right part of Fig. 6(B)). For patients who had hPG80 decrease after surgery (n = 46), the calculated p-value is $p < 0.0001$. For patients who had stable or increased hPG80 levels (n = 16), the p-value is p = 0.155. For all patients (n = 62), significant differences in median hPG80 levels were observed before and after surgery (5.36 pM versus 3.00 pM; $p < 0.0001$) (Fig. S11). 16 patients out of 46 patients (34.8%) who had a decreased level after surgery had hPG80 levels below the LoD (1.2 pM). An overall trend for declining hPG80 concentration was found from inclusion (median 3.08 pM; n = 194), through end of peri-operative chemotherapy (median 2.20 pM; n = 23), post-operative time (median 1.57 pM, n = 85), to the end of post-operative chemotherapy (median 1.21 pM, n = 6) (Fig. S12).

In the PRO-HCC cohort, individual concentration versus time curves of hPG80 evolved consistently with disease activity and AFP kinetics in most patients. This is illustrated by seven typical patient profiles (Figs. 7(A), S13 and S14). In particular, Fig. 7(A) illustrates a patient treated with nivolumab. For this patient, hPG80, present before the treatment, was undetectable upon complete response of the patient; upon relapse, hPG80 was again detected. The patients considered to be in remission after disease management had lower hPG80 levels, compared to those with active cancers (median 1.99 versus 15.71 pM, $p < 0.0001$, n = 63, Figs. S15A and 7(B)). Conversely, 76.0% of the patients whose disease progressed during treatments, had hPG80 increase >25%. Of note, AFP was not informative in 45.7% of patients, because the concentrations were below the most

Table 1
Patient demographic and clinical characteristics

Sample Status	No. of Patients	Gender*		Median Age, Years (range)	hPG80 Median (IQR), pM	hPG80 Mean (SE), pM	AJCC Stage (number of Patients)**			
		Male	Female				I	II	III	IV
All Cancer	1546	1042	470	66 (21-93)	4.88 (2.02-11.73)	12.94 (0.82)	233	246	210	777
Breast	62	0	62	57 (34-70)	2.5 (0.60-6.60)	6.35 (1.36)	41	12	2	6
CRC	305	174	123	64 (23-93)	4.36 (1.62-10.61)	10.29 (1.11)	25	73	27	169
Esophagus/Stomach	74	29	43	65 (21-83)	6.92 (3.00-19.08)	21.06 (6.25)	9	1	7	43
Kidney	184	135	48	64 (25-85)	7.25 (3.21-19.71)	21.50 (2.96)	5	19	15	144
Liver	110	82	23	65 (23-86)	11.65 (3.25-28.24)	17.76 (1.82)	4	28	43	24
Lung (NSCL)	60	39	21	67 (45-85)	5.78 (2.87-13.34)	10.39 (1.57)	30	21	8	1
Skin Melanoma	38	8	12	61 (38-79)	3.65 (1.65-7.62)	5.09 (0.79)	0	0	0	33
Ovary	44	0	44	60 (22-86)	3.18 (1.15-9.26)	10.39 (.571)	20	7	10	1
Pancreas	34	17	17	66 (30-83)	6.47 (5.13-11.98)	11.24 (2.38)	13	17	3	1
Prostate	558	558	0	70 (43-93)	4.59 (2.12-9.79)	11.58 (1.13)	46	47	91	353
Uterus (endometrium/cervix)	77	0	77	60 (29-90)	2.92 (0.90-6.91)	6.86 (1.39)	40	21	4	2
Sample Status	No. of Volonteers	Male	Female	Median Age, Years (range)	hPG80 Median (IQR), pM	hPG80 Mean (SE), pM				
Healthy blood donors	557	310	247	35 (18-70)	1.05 (0.00-2.92)	2.04 (0.11)				

* 34 missing gender (2.20%)
** 80 undetermined stage (5.12%)

commonly reported and used cut-off value of 20 ng/ml in clinical practice [19]. In these patients, significant relationships between hPG80 level changes and disease status at the end of treatments were found (median 1.47 pM for patients in remission versus 18.33 pM for those in progression, $p = 0.018$, Fig. S15B). We found no link between hPG80 and inflammation status, assessed by CRP concentration in the PRO-HCC cohort (Fig. S16) suggesting that, if any, impact of inflammation is probably limited.

4. Discussion

The data reported in the present paper demonstrate that hPG80 is overexpressed in the tumor, and present in the blood of the patient, not only in colorectal cancers as already known, but also in a wide range of 10 other epithelial and non-epithelial cancers.

There are evidence supporting the tumor origin of this expression. First, IHC revealed strong and specific hPG80 immunoreactivity in all the tumor tissue samples examined, regardless of the tumor origins, suggesting that hPG80 was ubiquitously expressed in all tested cancers. The hPG80-expressing cells were commonly found in the parenchyma, i.e. the epithelium for all organs, and occasionally in the stroma (connective tissue). In contrast, the tissues adjacent to the tumor bulks revealed no or minimum hPG80 expression, and in most cases, this extra-tumoral expression was found in the stroma. These results are in line with the work of Caplin et al. who detected the presence of hPG80 in liver and pancreatic cancers but not in normal liver and pancreas [20,21]. Caplin also showed that hPG80 did not mature into gastrin-NH2, as published for CRC and in agreement with the lack of secretion of gastrin-NH2 by CRC cell lines [20,21]. By contrast, in ovarian cancers, van Solinge et al. detected the biologically active gastrin-NH2 [22]. hPG80 was not detected as such. Thus, it is possible that in ovarian cancers, in addition to the presence and the release of hPG80 that is shown here *via* IHC and the consequence of hPG80 neutralization by a very specific antibody, part of hPG80 matures into gastrin-NH2 which could also be released. None of these studies however addressed the presence of hPG80 in the blood, described in the present study, nor the consequence of hPG80 neutralization in experimental models originating from these tumors.

Secondly, *in vitro* studies confirmed that hPG80 exhibited oncogenic functions on cancer stem cells by regulating sphere formations from cell lines originating from these tumors. Moreover, cancer patients had consistent significantly higher levels of hPG80 compared to healthy blood donors expected to be free of cancers even at early stage as examplified in the HCC cohort, thereby confirming the early role of hPG80 in tumorigenesis, in line with the IHC observations.

Two kinetic studies, where hPG80 was serially measured during cancer managements, confirmed that blood hPG80 level longitudinal changes were related to treatment efficacy and cancer activity. Our data confirm the previous work by Konturek et al., who first showed that blood hPG80 returned to control levels after surgical removal of colorectal tumors [23], but they extend the relevance of hPG80 to other cancer origins.

The ubiquitous overexpression of hPG80 found in the tumor and in the blood of cancer patients, regardless of the tumor origin, can be understood by the regulation of hPG80 expression related to some major oncogenic pathways, such as Wnt/β-catenin and RAS-RAF-ERK pathways. Indeed, the gene *GAST*, which encodes hPG80, is a target of these pathways, known to be overactivated in CRC and many other cancers, including those tested in the present studies [24–27]. Genetic abnormalities in these pathway genes have been well studied and characterized: *APC* and *CTNNB1* (β-catenin gene) mutations in the Wnt/β-catenin pathway, and *KRAS, B-RAF*, and *EGFR* (epidermal growth factor receptor) mutations in the RAS-ERK pathway [28,29]. The correlation found between blood hPG80 levels and tumor *GAST* mRNA expression in lung cancer patients strengthens this hypothesis.

If the present results establish that the tumor cells from many cancer types overexpress hPG80 and that hPG80 expression is related to cancer cell activity, some findings raise new questions and hypotheses. First, hPG80 was sometimes expressed in the tissues adjacent to the tumor. It is now recognized that regions surrounding tumors can exhibit morphological and phenotypical alterations with respect to non-tumor-bearing healthy tissues [30]. hPG80 expression in the tissues surrounding the tumor might indicate the presence of cancerous or precancerous lesions, that could potentially participate in tumor growth and progression. It would be interesting to examine the clinical outcomes of these patients to better define the clinical significance of hPG80 expression in tissues adjacent to the tumor. Indeed the expression of hPG80 in the tissues adjacent to the tumor might provide relevant information about the risk of subsequent recurrence. Interestingly, hPG80 expression was not restricted to epithelial cells, but was also detected in stromal cells as visualized in Fig. S8.

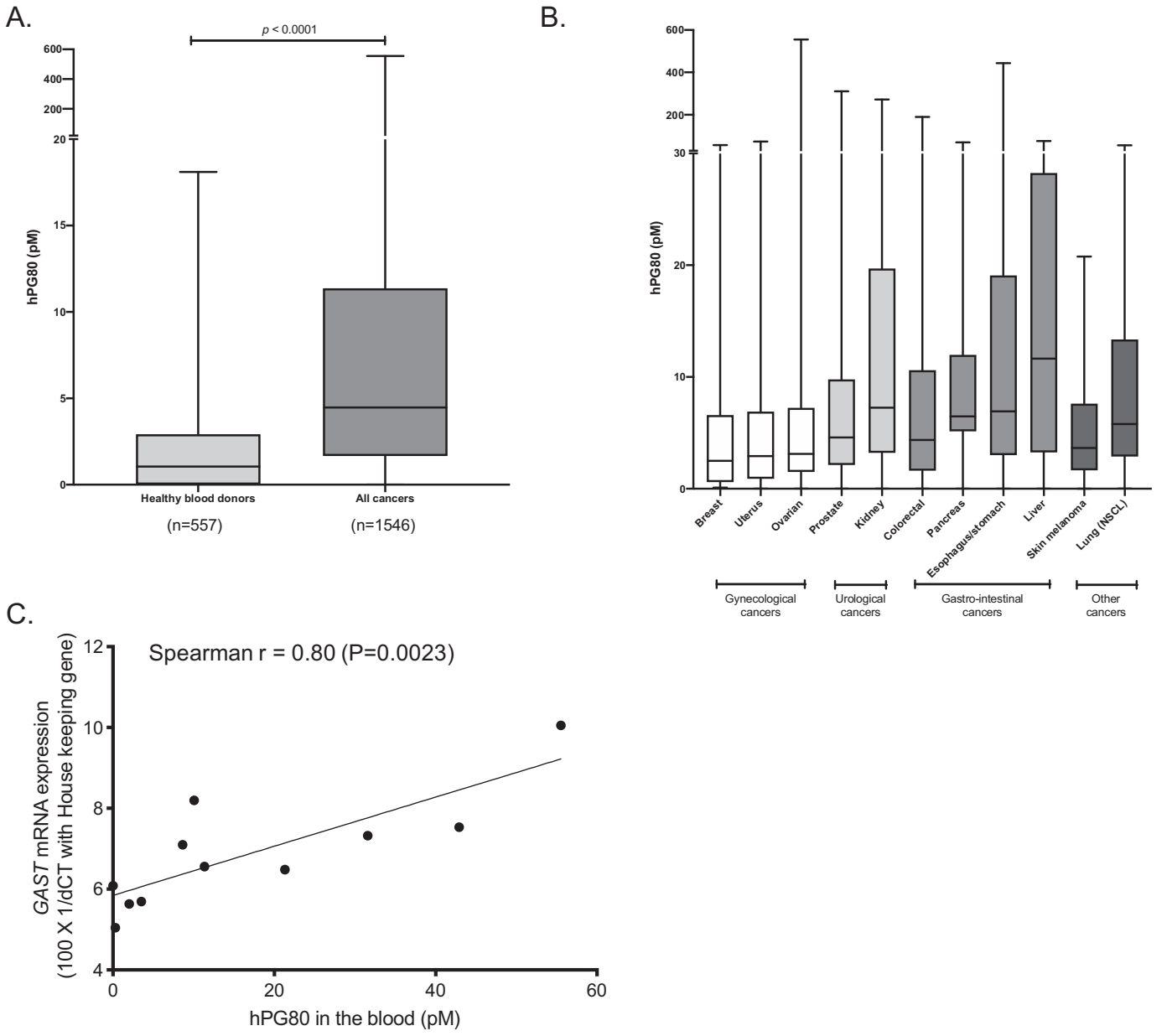

Fig. 5. hPG80 is detected in the blood of patients with various cancer origins. (A) Comparison of median hPG80 concentrations between healthy blood donors (n = 557) and cancer patients (n = 1546). (B) Comparison of median hPG80 concentrations between all types of cancers tested: breast (n = 62), CRC (n = 305), esophagus/stomach (n = 74), kidney (n = 184), liver (n = 110), lung (n = 60), skin melanoma (n = 38), ovary (n = 44), pancreas (n = 34), prostate (n = 558), uterus (n = 77). (C) Correlation between *GAST* mRNA tissue expression and hPG80 in the blood from the same lung cancer patient (n = 11).

The tumor stroma hosts many types of cells such as fibroblasts, vascular cells, and immune system cells. In waiting for the findings of further investigations about the origins of the cells that express hPG80 in the stroma, one hypothesis is that hPG80 would be expressed by fibroblasts. Indeed, tumor stroma fibroblasts, also known as cancer associated fibroblasts (CAFs) or myofibroblasts, are known to play a role in tumorigenesis, including tumor initiation and progression [31]. If this hypothesis was confirmed, it would be possible that expression of hPG80 in CAFs could modulate local tumor cell invasion and regulate tumor spreading to metastatic sites. In both tumor parenchyma and stroma, hPG80 was localized in the cytoplasm. In physiological conditions, within the antral G-cell, hPG80 is translated and folded into the endoplasmic reticulum, then transit throughout the trans-Golgi network before being packaged into immature secretory vesicles to undergo further cleavage [32]. We hypothesize that the punctate pattern of intracellular staining represents secretory granules in which neo-synthetized hPG80 is stored before being secreted. Our findings showing that anti-hPG80 neutralizing antibodies decreased *in vitro* cell proliferation and sphere formation of tumor cell lines confirmed that hPG80 is indeed released from tumor cells. Another possible source of blood hPG80 detected in cancer patients might be the G cells in the antrum of the stomach. One could hypothezise that hPG80 measured in the blood of cancer patients might come from these cells rather than from the tumor cells, emphasizing an endocrine secretion rather than a pathological one. A strong argument against this hypothesis is the fact that the expression of the *GAST* gene, encoding hPG80, decreases with age, which is not what is observed in cancer patients or even healthy blood donors since, as stated above, the relationship between hPG80 with age, if any, is a positive relationship [33–35].

A.

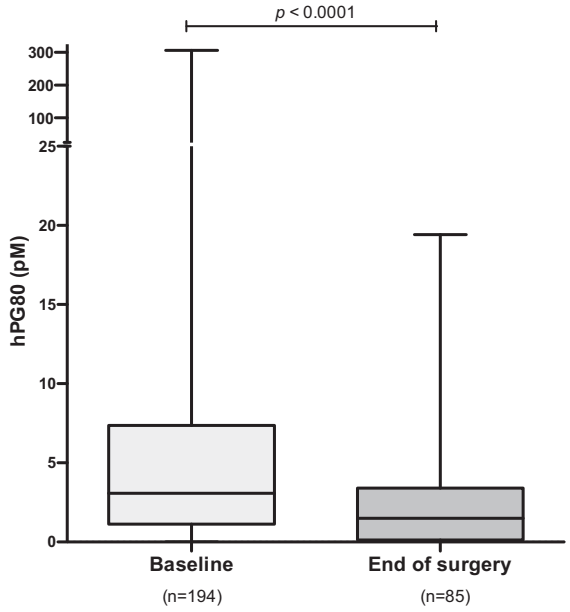

B.

hPG80 changes from baseline to post-operative time		
Decrease > -25%	Stable	Increase > +25%
74.2%	16.1%	9.7%

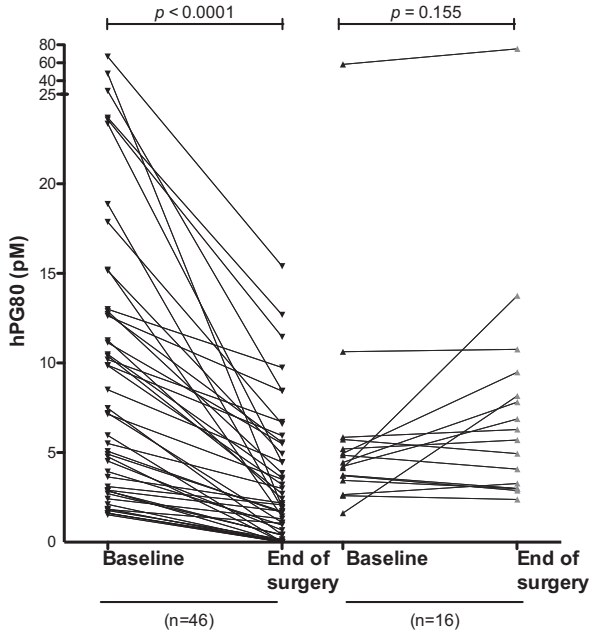

Fig. 6. hPG80 kinetics in patients receiving cancer treatments in the PRO-RENAPE cohort. Changes in hPG80 concentrations from baseline to post-operative time (8−24 h after surgery) in patients with peritoneal carcinomatoses from gastrointestinal cancers treated with cytoreductive surgery, with or without peri-operative chemotherapy. (A) hPG80 level changes at the population level (Baseline, $n = 194$; End of surgery, $n = 85$; $p < 0.0001$ with two-tailed Mann−Whitney U). (B) hPG80 level changes at individual levels. The left part of the Figure represents patients with decrease hPG80 between baseline and end of surgery ($n = 46$) and the right part of the Figure represents patients with stable or increase hPG80 ($n = 16$) between baseline and end of surgery ($p < 0.0001$ with Wilcoxon signed-rank). The table shows the proportions of patients who had hPG80 decline >25%, stable levels, and hPG80 increase >25%.

Of note, if this observation is consistent with the assumption of hPG80 secretion by cancer cells, it also raises therapeutic perspectives. Indeed, since sphere formation indicates the presence of cells with cancer stem cells (CSC) features, hPG80 coud be used as a target for future anti-hPG80 therapies. It was previously shown that anti-hPG80 antibodies decrease both *in vitro* and *in vivo* cancer stem cell frequency in colorectal cancer cell lines [5]. The present data suggest that similar results could be obtained in 5 other cancers from different origins and further studies will be required to evaluate for each individual type of cancer the risk and benefit of using anti-hPG80 as a treatment. Nevertheless, our data support the potential relevance of CSCs targeting, through hPG80, as a pan-cancer treatment strategy. Indeed, CSCs were identified in multiple malignancies including leukemia and different solid tumors, such as glioblastoma, breast and colon cancers [36], and have frequently been associated with chemoresistance and limited efficacy of standard anticancer therapies [37,38]. This is why therapies that target both CSCs and other more differentiated tumor cells are currently gaining attention within the scientific community. In that context, hPG80 represents an attractive potential therapeutic target due to its role in CSCs feature regulation in various cancer types [9]. A monoclonal humanized therapeutic antibody targeting hPG80 is being developed [5]. Furthermore, it has to be noted that similarly to hPG80, both *APC* and *KRAS* mutations promote CSC phenotype and disease dissemination in a mouse xenograft model [39]. This implies that hPG80 may act synergistically with Wnt and Ras pathways to support malignant transformation and activation of CSCs.

Moreover the data from the kinetic studies support the potential role of hPG80 as a monitoring marker of treatment efficacy. In the peritoneal carcinomatosis cancer patient cohort, hPG80 levels decreased significantly after surgery in 74.2% of the cases. In the remaining patients, the concomitant HIPEC (Hyperthermic Intraperitoneal Chemotherapy) might have induced an increase in hPG80 level in the remaining metastases since we previously described that chemotherapy induces hPG80 secretion [5]. Also, as illustrated with a HCC patient treated with nivolumab on Fig. 7(A), hPG80 reliably witnesses response to the treatment and disease evolution. Finally, blood hPG80 monitoring might also be considered as the future companion test for the monoclonal antibody on-development [5].

In summary, the data presented here show the potential value of hPG80 as a novel cancer target with potential strong important applications for cancer management. hPG80 could embody a new ubiquitous circulating tumor biomarker for monitoring disease activity and treatment efficacy in a wide spectrum of human malignancies, including the eleven frequent cancer origins tested here. It also represents a relevant target for a monoclonal antibody meant to improve anti-cancer therapeutic efficacy.

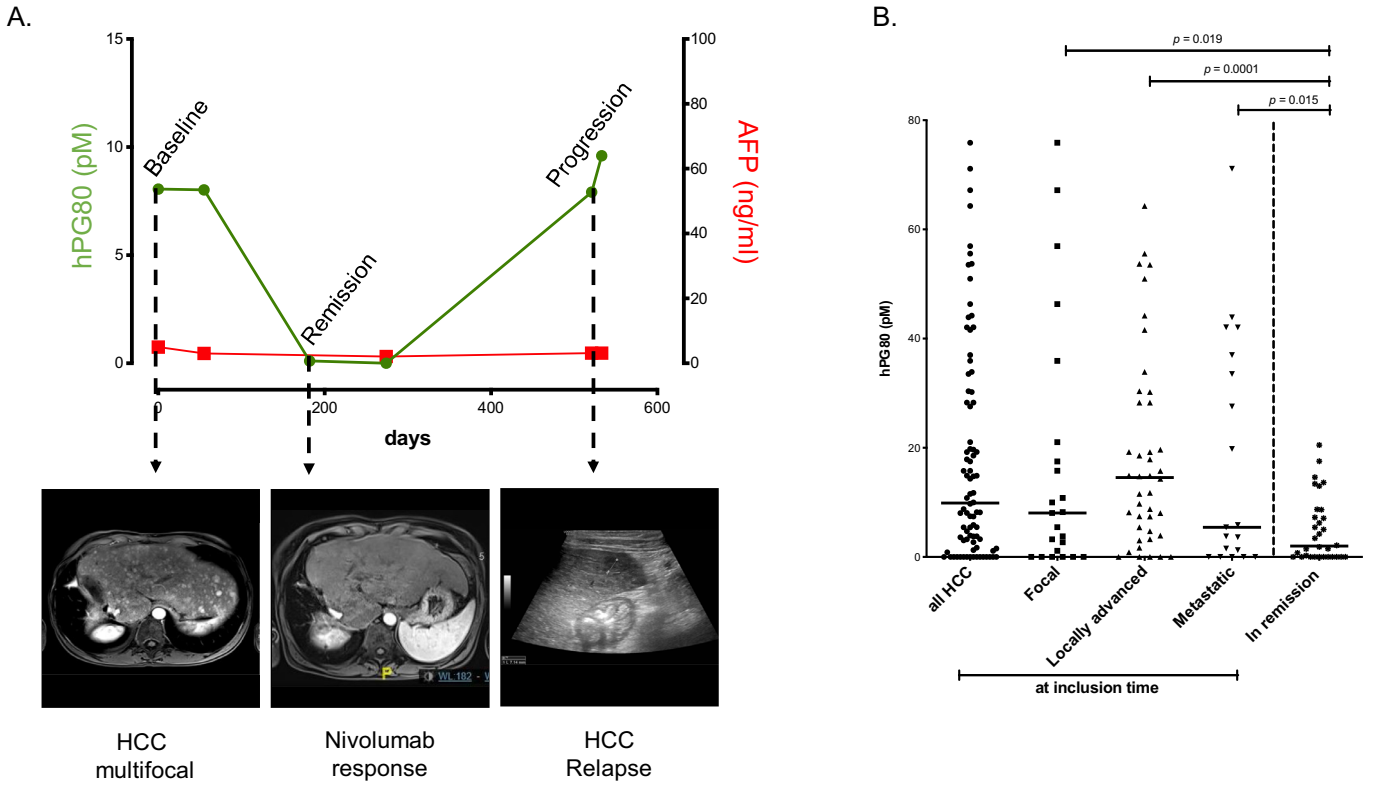

Fig. 7. hPG80 kinetics in patients receiving cancer treatments in the PRO-HCC cohort. (A) Illustrative hPG80 longitudinal changes around and during disease management (baseline; remission; progression), with associated imaging obtained at the same times (multifocal liver involvement at baseline; remission after treatment with nivolumab; new liver lesions on ultrasound at progression) in a typical patient. (B) hPG80 levels at different disease stages (focal, $n = 23$; locally advanced, $n = 42$; metastatic, $n = 19$) and at disease remission after treatment ($n = 32$). In order to simplify the reading of the graph, only statistically significant differences were shown on the graph. All the other comparisons were tested and none of them were significant.

Declaration of competing interest

AP and DJ own shares and are patent inventor in relation with this project.

DJ is a co-founder of the company and a senior scientific advisor.

AP is a co-founder of the company and the Chief Scientific Officer of the company.

All other authors: no conflict of interest.

Acknowledgments

The authors would like to thank all patients and their families, the investigators, study nurses, pharmacists, pathologists, and all study teams, especially the BIG-RENAPE collaborative group, The authors thank the Brest Biological Resources Center BB-0033-00037 (CRB Sante du CHRU de Brest) for providing high quality annotaded samples, especially Dr Pascale Marcorelles (Head of Anatomo-pathology department) and Dr Marie-Cecile Nicot (pharmacist) and the ECS-Progastrin team.

Funding sources

ECS-Progastrin.

Supplementary materials

Supplementary material associated with this article can be found in the online version at doi:10.1016/j.ebiom.2019.11.035.

References

[1] Rehfeld JF, Zhu X, Norrbom C, Bundgaard JR, Johnsen AH, Nielsen JE, et al. Prohormone convertases 1/3 and 2 together orchestrate the site-specific cleavages of progastrin to release gastrin-34 and gastrin-17. Biochem J 2008;415(1):35–43. Epub 2008/06/17. PubMed PMID: 18554181. doi: 10.1042/BJ20080881.

[2] Van Solinge WW, Nielsen FC, Friis-Hansen L, Falkmer UG, Rehfeld JF. Expression but incomplete maturation of progastrin in colorectal carcinomas. Gastroenterology 1993;104(4):1099–107. Epub 1993/04/01. PubMed PMID: 8462798.

[3] Koh TJ, Bulitta CJ, Fleming JV, Dockray GJ, Varro A, Wang TC. Gastrin is a target of the β-catenin/TCF-4 growth-signaling pathway in a model of intestinal polyposis. J Clin Invest 2000;106(4):533–9.

[4] Siddheshwar RK, Gray JC, Kelly SB. Plasma levels of progastrin but not amidated gastrin or glycine extended gastrin are elevated in patients with colorectal carcinoma. Gut 2001;48(1):47–52. Epub 2000/12/15. PubMed PMID: 11115822; PubMed Central PMCID: PMCPMC1728168. doi: 10.1136/gut.48.1.47.

[5] Prieur A, Cappellini M, Habif G, Lefranc MP, Mazard T, Morency E, et al. Targeting the wnt pathway and cancer stem cells with anti-progastrin humanized antibodies as a potential treatment for K-RAS-Mutated colorectal cancer. Clin Cancer Res 2017;23(17):5267–80. Epub 2017/06/11. PubMed PMID: 28600477. doi: 10.1158/1078-0432.CCR-17-0533.

[6] Hollande F, Lee DJ, Choquet A, Roche S, Baldwin GS. Adherens junctions and tight junctions are regulated via different pathways by progastrin in epithelial cells. J Cell Sci 2003;116:1187–97.

[7] Singh P, Owlia A, Varro A, Dai B, Rajaraman S, Wood T. Gastrin gene expression is required for the proliferation and tumorigenicity of human colon cancer cells. Cancer Res 1996;56(18):4111–5. Epub 1996/09/15. PubMed PMID: 8797575.

[8] Wu H, Owlia A, Singh P. Precursor peptide progastrin(1-80) reduces apoptosis of intestinal epithelial cells and upregulates cytochrome c oxidase Vb levels and synthesis of ATP. Am J Physiol Gastrointest Liver Physiol 2003;285(6):G1097–110.

[9] Giraud J, Failla LM, Pascussi JM, Lagerqvist EL, Ollier J, Finetti P, et al. Autocrine Secretion of Progastrin Promotes the Survival and Self-Renewal of Colon Cancer Stem-like Cells. Cancer Res 2016;76(12):3618–28.

[10] Najib S, Kowalski-Chauvel A, Do C, Roche S, Cohen-Jonathan-Moyal E, Seva C. Progastrin a new pro-angiogenic factor in colorectal cancer. Oncogene 2015;34(24):3120–30. Epub 2014/08/12. PubMed PMID: 25109333. doi: 10.1038/onc.2014.255.

[11] Katoh M, Katoh M. Molecular genetics and targeted therapy of WNT-related human diseases (Review). Int J Mol Med 2017;40(3):587–606. Epub 2017/07/22. PubMed PMID: 28731148; PubMed Central PMCID: PMCPMC5547940. doi: 10.3892/ijmm.2017.3071.
[12] White MC, Holman DM, Boehm JE, Peipins LA, Grossman M, Henley SJ. Age and cancer risk: a potentially modifiable relationship. Am J Prev Med 2014;46(3 Suppl 1):S7–15. Epub 2014/02/12. PubMed PMID: 24512933; PubMed Central PMCID: PMCPMC4544764. doi: 10.1016/j.amepre.2013.10.029.
[13] Mercier F, Hatton GI. Immunocytochemical basis for a meningeo-glial network. J Comp Neurol 2000;420(4):445–65. Epub 2000/05/11. PubMed PMID: 10805920.
[14] Hewitt SM, Baskin DG, Frevert CW, Stahl WL, Rosa-Molinar E. Controls for immunohistochemistry: the histochemical society's standards of practice for validation of immunohistochemical assays. J Histochem Cytochem 2014;62 (10):693–7. Epub 2014/07/16. PubMed PMID: 25023613; PubMed Central PMCID: PMCPMC4212362. doi: 10.1369/0022155414545224.
[15] Hussain M, Goldman B, Tangen C, Higano CS, Petrylak DP, Wilding G, et al. Prostate-specific antigen progression predicts overall survival in patients with metastatic prostate cancer: data from southwest oncology group trials 9346 (Intergroup study 0162) and 9916. J Clin Oncol 2009;27(15):2450–6. Epub 2009/04/22. PubMed PMID: 19380444; PubMed Central PMCID: PMCPMC2684851. doi: 10.1200/JCO.2008.19.9810.
[16] Singh P, Owlia A, Varro A, Dai B, Rajaraman S, Wood T. Gastrin gene expression is required for the proliferation and tumorigenicity of human colon cancer cells. Cancer Res 1996;56(18):4111–5.
[17] Lytle NK, Barber AG, Reya T. Stem cell fate in cancer growth, progression and therapy resistance. Nat Rev Cancer 2018;18(11):669–80. Epub 2018/09/20. PubMed PMID: 30228301. doi: 10.1038/s41568-018-0056-x.
[18] Weiswald LB, Bellet D, Dangles-Marie V. Spherical cancer models in tumor biology. Neoplasia 2015;17(1):1–15. Epub 2015/01/28. PubMed PMID: 25622895; PubMed Central PMCID: PMCPMC4309685. doi: 10.1016/j.neo.2014.12.004.
[19] Sarwar S, Khan AA, Tarique S. Validity of alpha fetoprotein for diagnosis of hepatocellular carcinoma in cirrhosis. J Coll Physicians Surg Pak 2014;24(1):18–22. Epub 2014/01/15. PubMed PMID: 24411536. doi: 01.2014/JCPSP.1822.
[20] Caplin M, Savage K, Khan K, Brett B, Rode J, Varro A, Dhillon A. Expression and processing of gastrin in pancreatic adenocarcinoma. Br J Surg 2000;87(8):1035–40.
[21] Caplin M, Khan K, Savage K, Rode J, Varro A, Michaeli D, et al. Expression and processing of gastrin in hepatocellular carcinoma, fibrolamellar carcinoma and cholangiocarcinoma. J Hepatol 1999;30(3):519–26. Epub 1999/04/06. PubMed PMID: 10190738.
[22] van Solinge WW, Odum L, Rehfeld JF. Ovarian cancers express and process progastrin. Cancer Res 1993;53(8):1823–8.
[23] Konturek P, Bielanski W, Konturek S, Hartwich A, Pierzchalski P, Gonciarz M, et al. Progastrin and Cyclooxygenase-2 in Colorectal Cancer. Dig Dis Sci 2002;47 (9):1984–91.
[24] Chakladar A, Dubeykovskiy A, Wojtukiewicz LJ, Pratap J, Lei S, Wang TC. Synergistic activation of the murine gastrin promoter by oncogenic ras and beta-catenin involves smad recruitment. Biochem Biophys Res Commun 2005;336(1):190–6. Epub 2005/09/06. PubMed PMID: 16139800. doi: 10.1016/j.bbrc.2005.08.061.
[25] Nakata H, Wang SL, Chung DC, Westwick JK, Tillotson LG. Oncogenic ras induces gastrin gene expression in colon cancer. Gastroenterology 1998;115(5):1144–53. Epub 1998/10/31. PubMed PMID: 9797369.
[26] Ghosh N, Hossain U, Mandal A, Sil PC. The wnt signaling pathway: a potential therapeutic target against cancer. Ann N Y Acad Sci 2019;1443(1):54–74. Epub 2019/04/25. PubMed PMID: 31017675. doi: 10.1111/nyas.14027.
[27] Khan AQ, Kuttikrishnan S, Siveen KS, Prabhu KS, Shanmugakonar M, Al-Naemi HA, et al. RAS-mediated oncogenic signaling pathways in human malignancies. Semin Cancer Biol 2019;54:1–13. Epub 2018/03/11. PubMed PMID: 29524560. doi: 10.1016/j.semcancer.2018.03.001.
[28] Malumbres M, Barbacid M. RAS oncogenes: the first 30 years. Nat Rev Cancer 2003;3(6):459–65. Epub 2003/06/05. PubMed PMID: 12778136. doi: 10.1038/nrc1097.
[29] Clevers H, Nusse R. Wnt/beta-catenin signaling and disease. Cell 2012;149 (6):1192–205. Epub 2012/06/12. PubMed PMID: 22682243. doi: 10.1016/j.cell.2012.05.012.
[30] Aran D, Camarda R, Odegaard J, Paik H, Oskotsky B, Krings G, et al. Comprehensive analysis of normal adjacent to tumor transcriptomes. Nat Commun 2017;8 (1):1077. Epub 2017/10/24. PubMed PMID: 29057876; PubMed Central PMCID: PMCPMC5651823. doi: 10.1038/s41467-017-01027-z.
[31] Liu T, Zhou L, Li D, Andl T, Zhang Y. Cancer-Associated fibroblasts build and secure the tumor microenvironment. Front Cell Dev Biol 2019;7:60. Epub 2019/05/21. PubMed PMID: 31106200; PubMed Central PMCID: PMCPMC6492564. doi: 10.3389/fcell.2019.00060.
[32] Bundgaard JR, Birkedal H, Rehfeld JF. Progastrin is directed to the regulated secretory pathway by synergistically acting basic and acidic motifs. J Biol Chem 2004;279(7):5488–93. Epub 2003/12/09. PubMed PMID: 14660571. doi: 10.1074/jbc.M310547200.
[33] Shan JH, Bai XJ, Han LL, Yuan Y, Sun XF. Changes with aging in gastric biomarkers levels and in biochemical factors associated with helicobacter pylori infection in asymptomatic chinese population. World J Gastroenterol 2017;23 (32):5945–53. Epub 2017/09/22. PubMed PMID: 28932086; PubMed Central PMCID: PMCPMC5583579. doi: 10.3748/wjg.v23.i32.5945.
[34] Chu KU, Evers BM, Ishizuka J, Beauchamp RD, Greeley Jr. GH, Townsend Jr. CM, et al. Short-term caloric restriction augments age-related decreases in gastrin content and release. Mech Ageing Dev 1996;87(1):25–33. Epub 1996/05/24. PubMed PMID: 8735904. doi: 10.1016/0047-6374(96)01695-8.
[35] Alfven G, Gustavsson P, Uvnas-Moberg K. Age-related decrease in plasma levels of gastrin, cholecystokinin and somatostatin. Acta Paediatr 1995;84(12):1344–6. Epub 1995/12/01. PubMed PMID: 8645948. doi: 10.1111/j.1651-2227.1995.tb13566.x.
[36] Prager BC, Xie Q, Bao S, Rich JN. Cancer stem cells: the architects of the tumor ecosystem. Cell Stem Cell 2019;24(1):41–53. Epub 2019/01/05. PubMed PMID: 30609398; PubMed Central PMCID: PMCPMC6350931. doi: 10.1016/j.stem.2018.12.009.
[37] Dawood S, Austin L, Cristofanilli M. Cancer stem cells: implications for cancer therapy. Oncology (Williston Park) 2014;28(12):1101–7. 10. Epub 2014/12/17. PubMed PMID: 25510809.
[38] Carnero A, Garcia-Mayea Y, Mir C, Lorente J, Rubio IT, ME LL. The cancer stem-cell signaling network and resistance to therapy. Cancer Treat Rev 2016;49:25–36. Epub 2016/07/20. PubMed PMID: 27434881. doi: 10.1016/j.ctrv.2016.07.001.
[39] Moon BS, Jeong WJ, Park J, Kim TI, Min do S, Choi KY. Role of oncogenic K-Ras in cancer stem cell activation by aberrant wnt/beta-catenin signaling. J Natl Cancer Inst 2014;106(2):djt373. Epub 2014/02/05. PubMed PMID: 24491301. doi: 10.1093/jnci/djt373.